Abdominal Radiology (2024) 49:3232–3240
https://doi.org/10.1007/s00261-024-04339-z

PELVIS

# Intravoxel incoherent motion diffusion-weighted imaging and dynamic contrast-enhanced MRI for predicting parametrial invasion in cervical cancer

Xin-xiang Li[1] · Bing Liu[2] · Ying Cui[1] · Yu-fei Zhao[1] · Yang Jiang[1] · Xin-gui Peng[1]

Received: 5 March 2024 / Revised: 11 April 2024 / Accepted: 15 April 2024 / Published online: 16 May 2024


## Abstract

**Purpose** This study aimed to assess the predictive efficacy of intravoxel incoherent motion diffusion-weighted imaging (IVIM-DWI) and dynamic contrast-enhanced magnetic resonance imaging (DCE-MRI) in parametrial invasion (PMI) in cervical cancer patients.

**Methods** A total of 83 cervical cancer patients (32 PMI-positive and 51 PMI-negative) retrospectively underwent pre-treatment IVIM-DWI and DCE-MRI scans. IVIM-DWI parameters included apparent diffusion coefficient (ADC), slow apparent diffusion coefficient (D), fast apparent diffusion coefficient (D*), and perfusion fraction (f). DCE-MRI parameters included volume transfer constant ($K^{trans}$), flux rate constant ($K_{ep}$), and fractional extravascular extracellular space volume ($V_e$). Logistic regression analyses were conducted to identify independent variables associated with PMI. Receiver operating characteristic curves were generated to assess the predictive performance of significant parameters.

**Results** Multivariable analysis revealed that the MRI parameters D (odds ratio [OR]: 7.05; 95% CI 1.78–27.88; $P=0.005$), D* (OR 6.58; 95% CI 1.49–29.10; $P=0.01$), f (OR 5.12; 95% CI 1.23–21.37; $P=0.03$), $K^{trans}$ (OR 4.60; 95% CI 1.19–17.81; $P=0.03$), and $K_{ep}$ (OR 4.90; 95% CI 1.25–19.18; $P=0.02$) were independent predictors of PMI in cervical cancer patients. The combined parameter incorporating these parameters demonstrated the highest performance in predicting PMI, yielding an area under the curve of 0.906, sensitivity of 84.4%, and specificity of 86.3%.

**Conclusion** The proposed combined parameter exhibited favorable performance in identifying PMI in cervical cancer patients.

✉ Xin-gui Peng
xingui2005peng@126.com

[1] Nurturing Center of Jiangsu Province for State Laboratory of AI Imaging & Interventional Radiology, Department of Radiology, Zhongda Hospital, School of Medicine, Southeast University, Nanjing 210009, China

[2] Department of Radiology, The First Affiliated Hospital of USTC, Division of Life Sciences and Medicine, University of Science and Technology of China, Hefei 230001, China

**Graphical abstract**

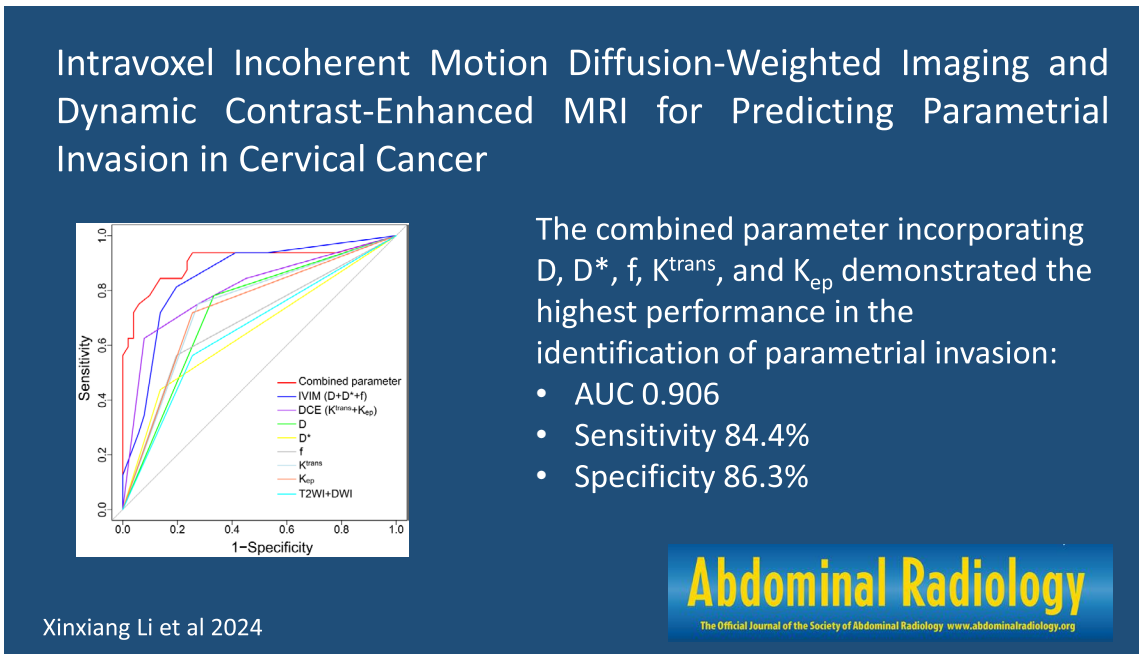


**Keywords** Cervical cancer · Parametrial invasion · Intravoxel incoherent motion · Diffusion weighted imaging · Dynamic contrast-enhanced

**Abbreviations**

| | |
|---|---|
| AUC | Area under the curve |
| DCE | Dynamic contrast-enhanced |
| DWI | Diffusion-weighted imaging |
| ICC | Intraclass correlation coefficient |
| IVIM | Intravoxel incoherent motion |
| MRI | Magnetic resonance imaging |
| PMI | Parametrial invasion |
| OR | Odds ratio |
| ROC | Receiver operating characteristic |
| ROI | Region of interest |

## Introduction

Cervical cancer is a common malignant tumor in the female reproductive system, posing a serious threat to women's health and lives [1]. The treatment of cervical cancer is closely related to its staging, and the chosen treatment modalities vary in clinical practice [2]. Patients without parametrial invasion (PMI) are generally treated with surgery, while those with PMI undergo concurrent chemoradiotherapy [3]. Additionally, PMI in cervical cancer is closely associated with postoperative recurrence, tumor metastasis, and overall survival [4, 5]. Therefore, the accurate pretreatment assessment of PMI in cervical cancer holds significant importance in clinical practice.

The quantitative imaging techniques of intravoxel incoherent motion diffusion weighted imaging (IVIM-DWI) and dynamic contrast-enhanced magnetic resonance imaging (DCE-MRI) can reveal the internal characteristics of tumors at the molecular level [6, 7]. IVIM-DWI can provide the information regarding histological perfusion and tumor angiogenesis on microcirculation without the use of contrast agents [8]. A previous study indicated that the pretreatment f value of IVIM-DWI was associated with treatment response in cervical cancer [9]. Furthermore, our previous study demonstrated that IVIM-DWI combined diffusion tensor imaging can predict the PMI in cervical cancer [10]. Additionally, DCE-MRI allows for the evaluation of vascular permeability, blood flow, and microcirculation within the tumor tissue [11–13]. DCE-MRI could predict the response of concurrent chemoradiotherapy in patients with locally advanced cervical cancer [14]. Similarly, our previous study demonstrated that DCE-MRI combined texture analysis can predict the PMI in cervical cancer [15].

Therefore, the objective of our current study was to assess the predictive value of IVIM-DWI and DCE-MRI for PMI in cervical cancer patients. The quantitative data obtained from the two technologies may increase the preoperative diagnostic accuracy of PMI in cervical cancer patients.

## Materials and methods

### Patients

Our institutional review board approved this study, and each patient signed an informed consent form (2021-RE-091). Ninety-six patients performed with radical hysterectomy, conforming cervical cancer with parametrial invasion, were admitted to our hospital between October 2017 and October 2019. IVIM-DWI and DCE-MRI examinations were conducted preoperatively for these patients. Exclusion criteria included: (a) patients with a history of treatment for cervical cancer before MRI ($n=5$); (b) insufficient image quality for further analysis ($n=5$); (c) more than two weeks between MRI and surgery ($n=3$). Finally, 83 patients were eligible for our study. The workflow of the patient selection was depicted in Fig. 1.

### Imaging acquisition

MRI data were obtained using a 3.0 T Signa HDxT scanner (GE Healthcare, USA). The scanning protocol contained T1-weighted imaging, T2-weighted imaging, diffusion-weighted imaging, IVIM-DWI, and DCE-MRI, which were performed with an 8-channel phased array body coil. IVIM was acquired using single-shot spin-echo echo planar imaging with 10 b values (0, 10, 20, 50, 100, 200, 400, 800, 1000, and 1200 s/mm$^2$). The scanning parameters of IVIM were as follows: repetition time, 4000 ms; echo time, 85 ms; slice thickness, 4 mm; field of view, 40 × 22 cm; matrix size, 130 × 128; and acquisition time, 5 min and 44 s.

DCE-MRI was conducted using a three-dimensional liver acceleration volume acquisition sequence. Before the injection of the contrast medium, three flip angles (5°, 10°, and 15°) were acquired. Patients received gadodiamide (Omniscan, GE Healthcare, USA) at a dosage of 0.1 mmol/kg, followed by a 20-mL saline flush. The protocol included the following parameters: repetition time of 4.2 ms, echo time of 2.2 ms, flip angle of 15°, slice thickness of 4 mm, field of view measuring 380 × 340 mm, matrix size of 320 × 224, time resolution of 7.0 s, a total of 43 phases, and a sampling time of 4 min and 40 s.

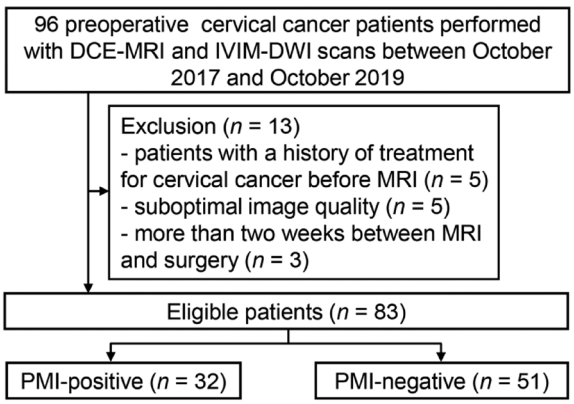


**Fig.1** The flowchart used in selection of the patients

### Imaging analysis

The IVIM-DWI data were post-processed using the functionality tools of GE Advantage Windows 4.5. The processing of the IVIM-DWI involved applying the bi-exponential model fitting formula, which is expressed as follows [16]: $S_b/S_0=(1-f)\exp(-b\times D)+f\exp(-b\times D^*)$, where $S_b$ denotes the mean signal intensity with the diffusion gradient b, and $S_0$ denotes the signal intensity at a b value of 0. Referring to the T2-weighted imaging, the maximum tumor area of IVIM images, demonstrating the most restricted diffusion, was delineated as the region of interest (ROI). ROIs were manually delineated, with the exclusion of necrosis, hemorrhage, cystic degeneration, and artifacts. Subsequently, the IVIM parameters (standard apparent diffusion coefficient [ADC], slow apparent diffusion coefficient [D], fast apparent diffusion coefficient [D*], and perfusion fraction [f]) were automatically generated. to cover as much of the tumor margin as possible.

Omni-Kinetics (O.K.; GE Healthcare, China) software was utilized to process the DCE-MRI data. The process of converting signal intensity into contrast agent concentration involved the use of multi-flip angle T1 mapping. A ROI was manually placed in the iliac artery to assess the arterial input function. The outlined tumor ROI slice was the same as IVIM. A modified Tofts model was used to generate the DCE-MRI parameters (volume transfer constant [$K^{trans}$], flux rate constant [$K_{ep}$], and fractional extravascular extracellular space volume [$V_e$]).

The diagnostic criteria for PMI on T2-weighted imaging were a disrupted cervical stromal ring with tiny nodular or irregular hyperintense signals extending to the parametrium. When using combined T2-weighted imaging and DWI (T2WI + DWI), the criteria were a hyperintense pattern on T2-weighted imaging, low signal intensity on an ADC map, and hyperintensity on DWI. A 5-point grading scale was employed to assess PMI presence: (1) definitely absent; (2) probably absent; (3) indeterminate; (4) probably present; and (5) definitely present. Grades 4 and 5 were considered positive for PMI on MRI, while grades 1 and 2 were deemed negative. Grade 3, indicating inconclusive results, was classified as negative.

IVIM-DWI and DCE-MRI were independently measured by two radiologists (Xinxiang Li, radiologist 1, and Xingui Peng, radiologist 2), with 12 and 20 years of experience in the gynecological system, respectively. IVIM-DWI

and DCE-MRI measurements were conducted twice within a week by radiologist 1 to determine intraobserver agreement. In order to evaluate interobserver agreement, the first measurement by radiologist 1 was compared with that obtained by radiologist 2. The value of the intraclass correlation coefficient (ICC) is greater than 0.75, indicating good agreement. Moreover, the DCE-MRI maps were integrated with the contrast-enhanced T1-weighted imaging images. The PMI from T2WI and T2WI + DWI were assessed by the same two radiologists. In instances of disagreement between the two radiologists, a collaborative review was conducted to reach a consensus for the final report.

### Statistical analysis

Continuous data were presented as median ± interquartile range. Univariable and multivariable logistic regression analyses were conducted to identify the MRI parameters significantly associated with PMI. Variables with a *P* value of less than 0.05 in the univariable analysis were included in the multivariable analysis, which identified the final variables through a stepwise backward process. Receiver operating characteristic curve analysis was employed to evaluate the predictive ability of IVIM-DWI and DCE-MRI variables in diagnosing PMI. The comparison of the area under the curve (AUC) was conducted using the DeLong test. The determination of cut-off values involved maximizing the Youden's index. In the assessment of data consistency, continuous variables were evaluated using the intraclass correlation coefficient, while categorical variables were assessed using κ statistics. A *P* value < 0.05 was regarded as statistically significant. Statistical analyses were conducted using SPSS software (version 26.0) and R software (version 4.2.2, http://www.r-project.org).

## Results

### Patient characteristic

The median age of the eligible patients was 50.0 (range: 44.8–58.5) years in the PMI-positive group and 50.0 (range: 46.0–55.0) years in the PMI-negative group. The final diagnosis revealed that 32 out of 83 (38.6%) cervical cancer patients were PMI-positive, while 51 out of 83 (61.4%) were PMI-negative. The clinical 2018 FIGO stage distribution was as follows: IB ($n=33$), IIA ($n=18$), IIB ($n=17$), IIIA ($n=8$), IIIB ($n=5$), and IIIC ($n=2$). The preoperative MRI parameters are listed in Table 1 and Fig. 2.

### Interobserver agreement

The intraobserver ICCs for ADC, D, D*, f, $K^{trans}$, $K_{ep}$, and $V_e$ measured by radiologist 1 ranged from 0.911 to 0.986. The interobserver ICCs for these parameters between radiologist 1 and radiologist 2 ranged from 0.926 to 0.991. Both intra- and interobserver ICCs indicated excellent agreement for these parameters (see Table 1). Therefore, the data analyzed were those obtained by radiologist 1, who had more experience in software usage. The interobserver consistency for

**Table 1** T2WI, IVIM-DWI and DCE-MRI parameters and their ICCs

| Parameters | PMI-positive ($n=32$) | PMI-negative ($n=51$) | j*P* value | ICC[#] | |
|---|---|---|---|---|---|
| | | | | Intraobserver (95% CI) | Interobserver (95% CI) |
| IVIM-DWI | | | | | |
| ADC ($\times 10^{-3}$ mm$^2$/s) | 0.785 (0.714–0.926) | 0.917 (0.792–1.036) | 0.003 | 0.899 (0.848, 0.933) | 0.849 (0.776, 0.900) |
| D ($\times 10^{-3}$ mm$^2$/s) | 0.657 (0.546–0.735) | 0.794 (0.678–0.842) | < 0.001 | 0.907 (0.835, 0.945) | 0.897 (0.836, 0.935) |
| D* ($\times 10^{-3}$ mm$^2$/s) | 27.95 (14.63–51.43) | 16.6 (11.6–31.5) | 0.03 | 0.917 (0.795, 0.958) | 0.879 (0.801, 0.924) |
| f | 0.243 (0.197–0.300) | 0.198 (0.165–0.229) | 0.004 | 0.877 (0.619, 0.945) | 0.833 (0.700, 0.902) |
| DCE-MRI | | | | | |
| $K^{trans}$, min$^{-1}$ | 0.320 (0.255–0.372) | 0.241 (0.188–0.278) | < 0.001 | 0.868 (0.736, 0.927) | 0.866 (0.482, 0.946) |
| $K_{ep}$, min$^{-1}$ | 0.596 (0.519–0.683) | 0.466 (0.390–0.565) | < 0.001 | 0.965 (0.944, 0.977) | 0.961 (0.940, 0.974) |
| $V_e$ | 0.581 (0.484–0.676) | 0.518 (0.457–0.584) | 0.01 | 0.956 (0.930, 0.972) | 0.951 (0.925, 0.968) |
| T2WI (+)/(-) | 14 (43.8)/18 (56.3) | 15 (29.4)/36 (70.6) | 0.24 | | 0.841 (0.719, 0.963) |
| T2WI + DWI (+)/(−) | 18 (56.3)/14(43.8) | 13 (25.5)/38 (74.5) | 0.005 | | 0.870 (0.760, 0.980) |

*CI*, confidence intervals, *DCE-MRI* dynamic contrast-enhanced magnetic resonance imaging, $V_e$ fractional extravascular extracellular space volume, *ICC* intraclass correlation coefficient, *IVIM-DWI* intravoxel incoherent motion diffusion weighted imaging, $D^*$ fast apparent diffusion coefficient, *PMI* parametrial invasion, *f* perfusion fraction, *D* slow apparent diffusion coefficient, *ADC* standard apparent diffusion coefficient, $K_{ep}$ the flux rate constant, $K^{trans}$ the volume transfer constant. (+)/(−) represent parametrial invasion positive/negative identified by MRI

#Categorical variables were analyzed using κ statistics and continuous variables were analyzed using intraclass correlation coefficient

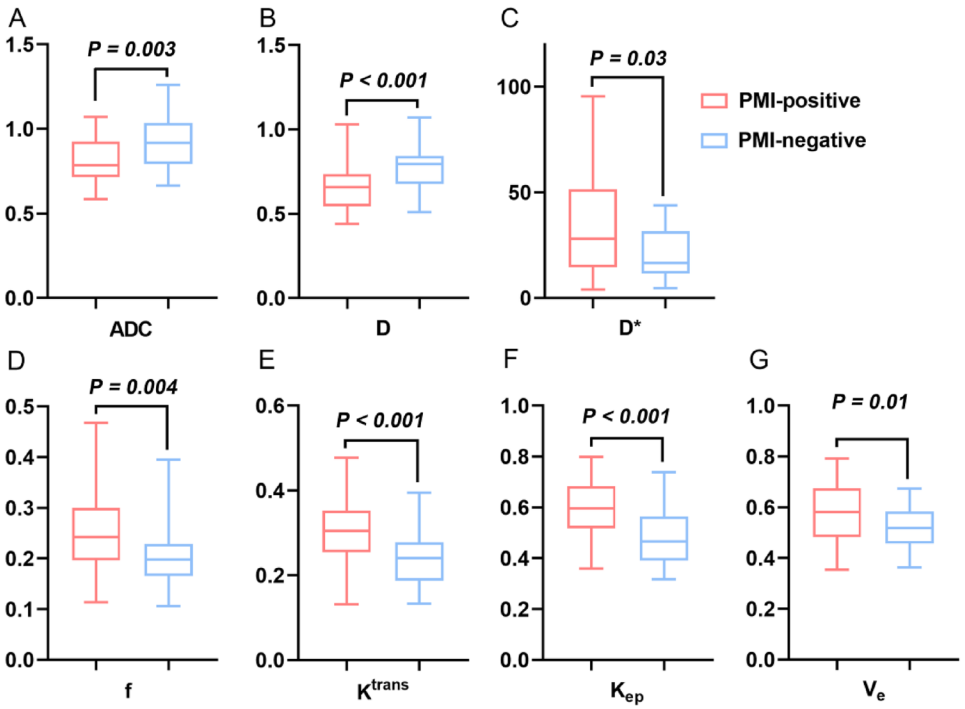


**Fig. 2** Boxplots of IVIM-DWI (ADC, D, D*, and f) and DCE-MRI ($K^{trans}$, $K_{ep}$, and $V_e$) between PMI-positive and PMI-negative groups

T2WI and T2WI + DWI in these cases was 0.841 and 0.870, respectively. The κ statistic value also indicated excellent agreement**.**

## IVIM-DWI and DCE-MRI parameters associated with parametrial invasion: uni- and multivariable analyses

Variables with a significance level below 0.05 in the univariable analysis were deemed to be associated with PMI. The MRI parameters statistically related with PMI contained ADC (OR 4.27; 95% CI 1.66–11.00; $P = 0.003$), D (OR 7.14; 95% CI 2.57–19.82; $P < 0.001$), D* (OR 4.89; 95% CI 1.70–14.11; $P = 0.003$), f (OR 5.27; 95% CI 1.97–14.08; $P = 0.001$), $K^{trans}$ (OR 7.93; 95% CI 2.89–21.75; $P < 0.001$), $K_{ep}$ (OR 7.47; 95% CI 2.76–20.21; $P < 0.001$), and $V_e$ (OR 5.55; 95% CI 1.93–15.97; $P = 0.001$) (see Table 2).

Subsequently, a multivariable analysis employing a stepwise backward procedure was conducted to ascertain variables from the univariable analysis that could potentially contribute to distinguishing patients with PMI. Consequently, D (OR 7.05; 95% CI 1.78–27.88; $P = 0.005$), D* (OR 6.58; 95% CI 1.49–29.10; $P = 0.01$), f (OR 5.12; 95% CI 1.23–21.37; $P = 0.03$), $K^{trans}$ (OR 4.60; 95% CI 1.19–17.81; $P = 0.03$), and $K_{ep}$ (OR 4.90; 95% CI 1.25–19.18; $P = 0.02$)

**Table 2** MRI parameters associated with cervical cancer with parametrial invasion: uni- and multivariable analyses

| Parameters | Univariable analysis | | | Multivariable analysis | | |
|---|---|---|---|---|---|---|
| | Coefficient | OR (95% CI) | *P* Value | Coefficient | OR (95% CI) | *P* Value |
| Intercept | | | | − 4.21 | | < 0.001 |
| ADC | 1.45 | 4.27 (1.66, 11.00) | 0.003 | − 0.34 | 0.71 (0.14, 3.59) | 0.68 |
| D | 1.97 | 7.14 (2.57, 19.82) | < 0.001 | 1.95 | 7.05 (1.78, 27.88) | 0.005 |
| D* | 1.59 | 4.89 (1.70, 14.11) | 0.003 | 1.88 | 6.58 (1.49, 29.10) | 0.01 |
| f | 1.66 | 5.27 (1.97, 14.08) | 0.001 | 1.63 | 5.12 (1.23, 21.37) | 0.03 |
| $K^{trans}$ | 2.07 | 7.93 (2.89, 21.75) | < 0.001 | 1.53 | 4.60 (1.19, 17.81) | 0.03 |
| $K_{ep}$ | 2.01 | 7.47 (2.76, 20.21) | < 0.001 | 1.59 | 4.90 (1.25, 19.18) | 0.02 |
| $V_e$ | 1.71 | 5.55 (1.93, 15.97) | 0.001 | 0.67 | 1.95 (0.42, 9.06) | 0.39 |

*CI* confidence intervals, $V_e$ fractional extravascular extracellular space volume, *ICC* intraclass correlation coefficient, $D^*$ fast apparent diffusion coefficient, *OR* odds ratio, *f* perfusion fraction, *D* slow apparent diffusion coefficient, *ADC* standard apparent diffusion coefficient, $K_{ep}$ the flux rate constant, $K^{trans}$ the volume transfer constant

were identified as independent factors associated with PMI (see Table 2).

### Predictive performance of IVIM-DWI and DCE-MRI parameters

According to the Youden's index, the cutoff values for the parameters of D, D*, f, $K^{trans}$, and $K_{ep}$ were determined as $0.740\times10^{-3}$ $mm^2/s$, $35.5\times10^{-3}$ $mm^2/s$, 0.236, 0.268 $min^{-1}$, and 0.561 $min^{-1}$, respectively. ROC analyses revealed that the AUCs for D, D*, f, $K^{trans}$, and $K_{ep}$ were 0.724, 0.650, 0.683, 0.738, and 0.732, respectively. When compared with T2WI + DWI (AUC: 0.654), IVIM and DCE suggested higher predictive ability, with an AUC of 0.849 and 0.806, respectively (Delong test *P* values of 0.004 and 0.04, respectively). Moreover, comparing with T2WI + DWI, individual parameters (D, D*, f, $K^{trans}$, $K_{ep}$), IVIM (D + D* + f), and DCE ($K^{trans}$ + $K_{ep}$), we found that the combined parameter (D + D* + f + $K^{trans}$ + $K_{ep}$) achieved the highest AUC of 0.906 (Fig. 3). The Delong test showed that all *P* values were < 0.05 when comparing the combined parameters with each individual parameter. The combined parameter enabled the identification of PMI with a sensitivity of 84.4% (27 of 32) and a specificity of 86.3% (44 of 51). IVIM identified 81.3% sensitivity (26 of 32) and 80.4% specificity (41 of 51) for PMI, while DCE identified 62.5% sensitivity (20 of 32) and 92.2% specificity (47 of 51) for parametrial invasion. The diagnostic abilities of these independent predictors of PMI are tabulated in Table 3. Representative IVIM-DWI and DCE-MRI images of a patient with cervical cancer are shown in Fig. 4.

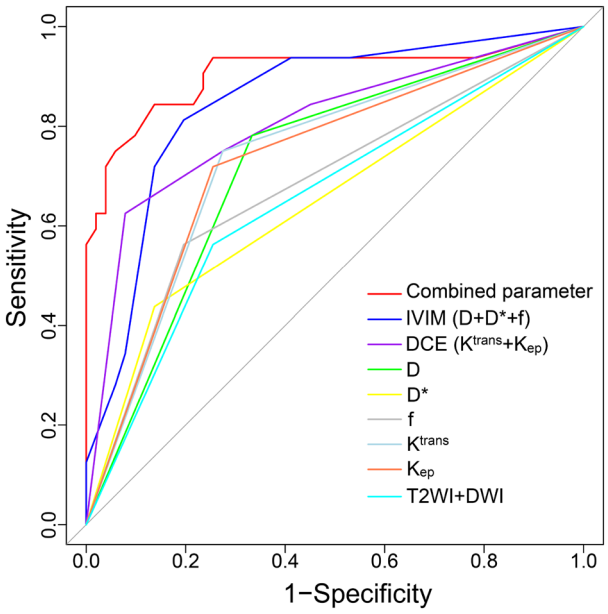


**Fig. 3** Receiver operating characteristic curves of D, D*, f, $K^{trans}$, $K_{ep}$, IVIM, DCE, and combined parameter in predicting cervical cancer with parametrial invasion

## Discussion

In our study, the multivariable analysis suggested that D, D*, f, $K^{trans}$, and $K_{ep}$ were independent factors associated with parametrial invasion. The combined parameter, which integrated these variables, exhibited the highest predictive performance for parametrial invasion in cervical cancer patients, achieving an AUC of 0.906, sensitivity of 84.4%, and specificity of 86.3%.

**Table 3** Performance of the IVIM-DWI and DCE-MRI parameters in predicting cervical cancer with parametrial invasion

| Parameters | Cut-off value | AUC (95% CI) | Sensitivity (%) | Specificity (%) | *P* value |
|---|---|---|---|---|---|
| Combined parameter | | 0.906 (0.826,0.986) | 84.4 | 86.3 | |
| IVIM (D + D* + f) | | 0.849 (0.763, 0.936) | 81.3 | 80.4 | 0.04† |
| DCE ($K^{trans}$ + $K_{ep}$) | | 0.806 (0.707, 0.906) | 62.5 | 92.2 | 0.02† |
| D | 0.740 | 0.724 (0.626, 0.822) | 78.1 | 66.7 | < 0.001$ |
| D* | 35.5 | 0.650 (0.551, 9,750) | 43.8 | 86.3 | < 0.001$ |
| f | 0.236 | 0.683 (0.580, 0.786) | 56.3 | 80.4 | < 0.001$ |
| $K^{trans}$ | 0.268 | 0.738 (0.640, 0.836) | 75.0 | 72.5 | < 0.001# |
| $K_{ep}$ | 0.561 | 0.732 (0.632, 0.831) | 71.9 | 74.5 | < 0.001# |
| T2WI + DWI | | 0.654 (0.548, 0.760) | 56.3 | 74.5 | < 0.001§ |

*AUC* area under receiver operating characteristic, *CI* confidence intervals, *DCE* dynamic contrast-enhanced, *IVIM* intravoxel incoherent motion, $D^*$ fast apparent diffusion coefficient, *f* perfusion fraction, *D* slow apparent diffusion coefficient, $K_{ep}$ the flux rate constant, $K^{trans}$ the volume transfer constant

#Represent DCE vs. $K^{trans}$ and $K_{ep}$, respectively

$Represent IVIM vs. D, D* and f, respectively

†Represent combined parameter vs. IVIM and DCE, respectively

§Represents combined parameter vs. T2WI combined DWI

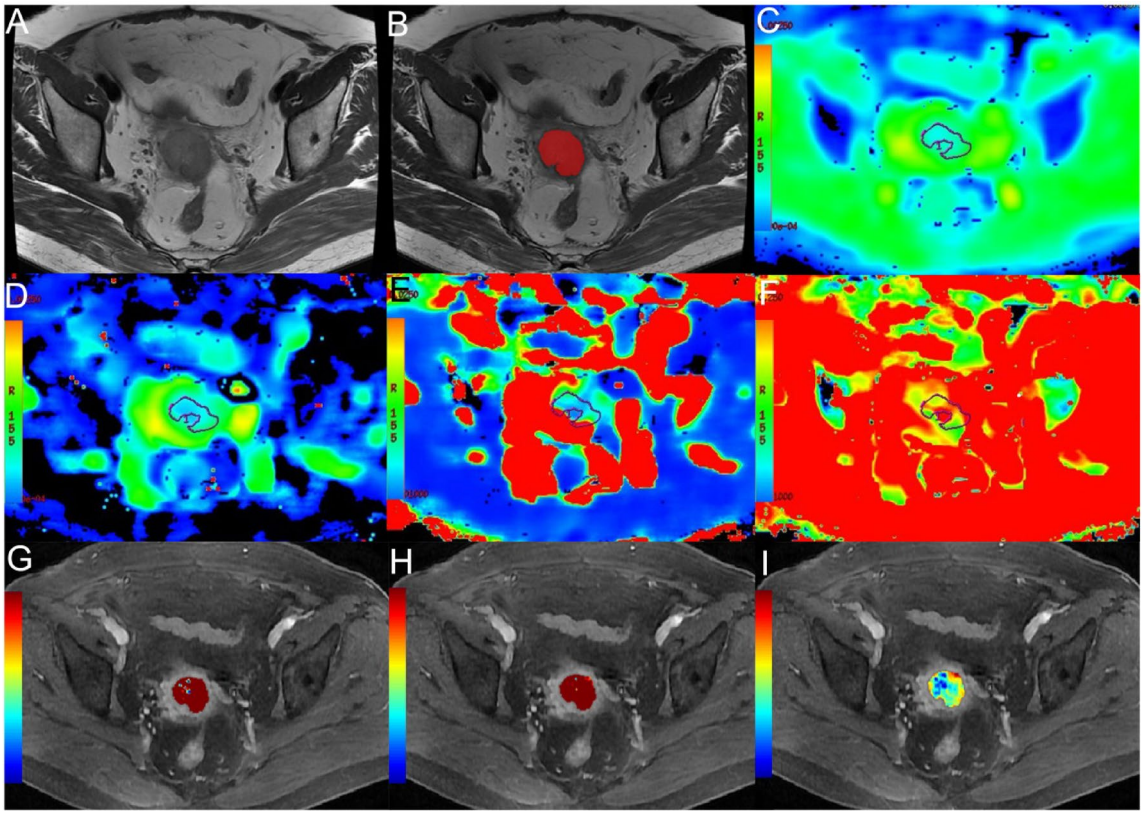


**Fig. 4** A 52-year-old woman diagnosed with stage IIB cervical cancer. **A** and **B** T2-weighted images reveal a slightly hyperintense cervical mass. **C–F** ADC, D, D*, and f parametric maps are obtained from IVIM-DWI, with corresponding values of 0.958 × 10–3 $mm^2/s$, $0.825 \times 10^{-3}$ $mm^2/s$, $95.4 \times 10^{-3}$ $mm^2/s$, and 0.241, respectively. **G–I** Parametric maps of $K^{trans}$, $K_{ep}$, and $V_e$ are derived from DCE-MRI, with corresponding values of 0.425 $min^{-1}$, 0.582 $min^{-1}$, and 0.460

Utilizing multiple b-values and based on a bi-exponential model, IVIM-DWI provides insights into tumor water molecule diffusion, tumor angiogenesis, and tissue perfusion through various parameters [17, 18]. In our investigation, we observed a decrease in the D value within the PMI-positive group compared to the PMI-negative group. The D value, which excludes the low b-value perfusion component, portrays the intrinsic characteristics of water molecule diffusion within the tumor [19]. Greater intercellular space in tumor cells correlates with faster water molecule diffusion [19].

Hence, our results suggest that the intercellular space within tumor cells of the PMI-positive group is diminished in contrast to the PMI-negative group. This discrepancy may stem from the more prominent non-directional growth characteristic of tumor cells in the PMI-positive group, indirectly reflecting increased malignancy level in cervical cancer with parametrial invasion. Additionally, our study revealed that both D* and f values exhibited an elevation within the PMI-positive group when contrasted with the PMI-negative group. This indicates a greater quantity or density of vascular generation in cervical cancer with parametrial invasion compared to those without.

DCE-MRI enables quantitative assessment of tissue microcirculation characteristics, including tumor angiogenesis, permeability, heterogeneity, and spatial distribution [20–22]. In our current study, DCE-MRI parameters $K^{trans}$ and $K_{ep}$ were observed to be higher values in the PMI-positive group in comparison with the PMI-negative group. This suggests greater tumor angiogenesis and vascular density in the parametrial invasion of cervical cancer. Furthermore, it is well-established that cervical cancer with parametrial invasion tends to be at a higher stage than those without parametrial invasion [23], indicating an increased vascular generation with advanced cervical cancer stages. Prior research has associated high $K_{ep}$ values with poor outcomes in cervical cancer patients [24], suggesting an association between $K_{ep}$ values and the malignant behavior of cervical cancer. Consistent with our findings, which link high $K_{ep}$ values to malignant behavior, i.e., parametrial invasion. More importantly, the identification of parametrial invasion in cervical cancer using IVIM and DCE, as well as their combined parameters, was superior to T2WI + DWI in our study, indicating the clinical feasibility of applying IVIM and DCE.

It is important to acknowledge several limitations of the present study. Firstly, IVIM-DWI and DCE-MRI scans were not conducted on every hospitalized cervical cancer patient, which could introduce bias. Secondly, this study is a single-center study with a relatively small sample size. Consequently, in future research, a multi-center study will be conducted to collect a larger sample for further investigation. Thirdly, radiologists manually delineated the regions of interest in the study, potentially introducing subjective factors and variability in both inter- and intraobserver measurements, as well as bias in slice selection.

In conclusion, the combined parameter comprising D, D*, f, $K^{trans}$, and $K_{ep}$ demonstrated favorable predictive performance in identifying parametrial invasion in cervical cancer patients. IVIM-DWI and DCE-MRI could offer valuable guidance in treatment decisions and the management of cervical cancer patients.

**Author contributions** Conception and design: X.X.L., X.G.P.; Administrative support: X.G.P.; Provision of study materials or patients: X.X.L., B.L., X.G.P.; Collection and assembly of data: X.X.L., B.L., Y.C., X.G.P.; Data analysis and interpretation: X.X.L., Y.J., Y.F.Z.; Manuscript writing: All authors; Final approval of manuscript: All authors.

**Funding** This study has received funding by National Natural Science Foundation of China (82272064), Jiangsu Provincial Science and Technique Program (BK20221461), Postgraduate Research & Practice Innovation Program of Jiangsu Province (KYCX21_0159, KYCX22_0297 and KYCX23_0323).

## Declarations

**Conflict of interest** The authors declare that they have no conflict of interest.

**Ethical approval** The study protocol was approved by the institutional review board (2021-RE-091).

## References

1. Perkins RB, Wentzensen N, Guido RS, Schiffman M. Cervical cancer screening: A review. JAMA 2023;330:547.
2. Bhatla N, Aoki D, Sharma DN, Sankaranarayanan R. Cancer of the cervix uteri. International Journal of Gynecology & Obstetrics 2018;143:22-36.
3. Cohen PA, Jhingran A, Oaknin A, Denny L. Cervical cancer. Lancet 2019;393:169-182.
4. Nakamura K, Joja I, Nagasaka T, Fukushima C, Kusumoto T, Seki N, et al. The mean apparent diffusion coefficient value (ADC-mean) on primary cervical cancer is a predictive marker for disease recurrence. Gynecologic Oncology 2012;127:478-483.
5. Russo L, Pasciuto T, Lupinelli M, Urbano A, D'Erme L, Amerighi A, et al. The value of MRI in quantification of parametrial invasion and association with prognosis in locally advanced cervical cancer: the "PLACE" study. European Radiology 2023.
6. Lin M, Yu X, Chen Y, Ouyang H, Wu B, Zheng D, et al. Contribution of mono-exponential, bi-exponential and stretched exponential model-based diffusion-weighted MR imaging in the diagnosis and differentiation of uterine cervical carcinoma. European Radiology 2016;27:2400-2410.
7. Wang W, Fan X, Yang J, Wang X, Gu Y, Chen M, et al. Preliminary MRI study of extracellular volume fraction for identification of lymphovascular space invasion of cervical cancer. Journal of Magnetic Resonance Imaging 2022;57:587-597.
8. Kim B, Lee SS, Sung YS, Cheong H, Byun JH, Kim HJ, et al. Intravoxel incoherent motion diffusion-weighted imaging of the pancreas: Characterization of benign and malignant pancreatic pathologies. Journal of Magnetic Resonance Imaging 2017;45:260-269.
9. Perucho JAU, Wang M, Vardhanabhuti V, Tse KY, Chan KKL, Lee EYP. Association between IVIM parameters and treatment response in locally advanced squamous cell cervical cancer treated by chemoradiotherapy. European Radiology 2021;31:7845-7854.
10. Lin T-T, Li X-X, Lv W-F, Dong J-N, Wei C, Wang T-T, et al. Diagnostic value of combined intravoxel incoherent motion diffusion-weighted magnetic resonance imaging with diffusion tensor imaging in predicting parametrial infiltration in cervical cancer. Contrast Media & Molecular Imaging 2021;2021:1-7.
11. Guljaš S, Dupan Krivdić Z, Drežnjak Madunić M, Šambić Penc M, Pavlović O, Krajina V, et al. Dynamic contrast-enhanced study in the mpMRI of the prostate—Unnecessary or underutilised? A narrative review. Diagnostics 2023;13:3488.
12. Li X, Huang W, Holmes JH. Dynamic contrast-enhanced (DCE) MRI. Magnetic Resonance Imaging Clinics of North America 2024;32:47-61.
13. Song J, Hu Q, Ma Z, Zhang J, Chen T. Value of diffusion-weighted and dynamic contrast-enhanced MR in predicting parametrial invasion in cervical stromal ring focally disrupted stage IB–IIA cervical cancers. Abdominal Radiology 2019;44:3166-3174.
14. Zhang Q, Guo J, Ouyang H, Chen S, Zhao X, Yu X. Added-value of dynamic contrast-enhanced MRI on prediction of tumor recurrence in locally advanced cervical cancer treated with chemoradiotherapy. European Radiology 2022;32:2529-2539.
15. Li X-x, Lin T-t, Liu B, Wei W. Diagnosis of cervical cancer with parametrial invasion on whole-tumor dynamic contrast-enhanced magnetic resonance imaging combined with whole-lesion texture analysis based on T2-weighted images. Frontiers in Bioengineering and Biotechnology 2020;8.
16. Zhang Y, Sheng R, Yang C, Dai Y, Zeng M. The feasibility of using Tri-exponential intra-voxel incoherent motion DWI for identifying the microvascular invasion in hepatocellular carcinoma. Journal of Hepatocellular Carcinoma 2023;10:1659-1671.
17. Noij DP, Martens RM, Marcus JT, de Bree R, Leemans CR, Castelijns JA, et al. Intravoxel incoherent motion magnetic resonance imaging in head and neck cancer: A systematic review of the diagnostic and prognostic value. Oral Oncology 2017;68:81-91.
18. Iima M, Le Bihan D. Clinical intravoxel incoherent motion and diffusion MR imaging: Past, present, and future. Radiology 2016;278:13-32.
19. Wang YXJ, Huang H, Zheng CJ, Xiao BH, Chevallier O, Wang W. Diffusion-weighted MRI of the liver challenges and some solutions for the quantification of apparent diffusion coefficient and intravoxel incoherent motion. American Journal of Nuclear Medicine and Molecular Imaging 2021;11:107-142.
20. Bol K, Haeck JC, Groen HC, Niessen WJ, Bernsen MR, de Jong M, et al. Can DCE-MRI explain the heterogeneity in radiopeptide uptake imaged by SPECT in a pancreatic neuroendocrine tumor model? PloS One 2013;8:e77076.
21. Heye AK, Culling RD, Valdes Hernandez Mdel C, Thrippleton MJ, Wardlaw JM. Assessment of blood-brain barrier disruption

using dynamic contrast-enhanced MRI: A systematic review. NeuroImage Clinical 2014;6:262-274.
22. Hylton N. Dynamic contrast-enhanced magnetic resonance imaging as an imaging biomarker. Journal of Clinical Oncology 2006;24:3293-3298.
23. Cibula D, Potter R, Planchamp F, Avall-Lundqvist E, Fischerova D, Haie-Meder C, et al. The European Society of Gynaecological Oncology/European Society for Radiotherapy and Oncology/European Society of Pathology Guidelines for the Management of Patients with Cervical Cancer. Virchows Archiv: International Journal of Pathology 2018;472:919-936.
24. Lund KV, Simonsen TG, Kristensen GB, Rofstad EK. Pharmacokinetic analysis of DCE-MRI data of locally advanced cervical carcinoma with the Brix model. Acta Oncologica 2019;58:828-837.